Available online at www.sciencedirect.com

ScienceDirect

Journal of Nutritional Biochemistry 50 (2017) 74–82

Journal of Nutritional Biochemistry

Nutrient sensing and metabolic changes after methionine deprivation in primary muscle cells of turbot (*Scophthalmus maximus* L.)☆,☆☆

Haowen Jiang, Fuyun Bian, Huihui Zhou, Xuan Wang, Kaidi Wang, Kangsen Mai, Gen He*

Key Laboratory of Aquaculture Nutrition (Ministry of Agriculture), Ocean University of China, 5 Yushan Road, Qingdao 266003, China

Received 12 January 2017; received in revised form 11 April 2017; accepted 29 August 2017

Abstract

The low methionine content in plant-based diets is a major limiting factor for feed utilization by animals. However, the molecular consequences triggered by methionine deficiency have not been well characterized, especially in fish species, whose metabolism is unique in many aspects and important for aquaculture industry. In the present study, the primary muscle cells of turbot (*Scophthalmus maximus* L.) were isolated and treated with or without methionine for 12 h in culture. The responses of nutrient sensing pathways, the proteomic profiling of metabolic processes, and the expressions of key metabolic molecules were systematically examined. Methionine deprivation (MD) suppressed target of rapamycin (TOR) signaling, activated AMP-activated protein kinase (AMPK) and amino acid response (AAR) pathways. Reduced cellular protein synthesis and increased protein degradation by MD led to increased intracellular free amino acid levels and degradations. MD also reduced glycolysis and lipogenesis while stimulated lipolysis, thus resulted in decreased intracellular lipid pool. MD significantly enhanced energy expenditure through stimulated tricarboxylic acid (TCA) cycle and oxidative phosphorylation. Collectively, our results identified a comprehensive set of transcriptional, proteomic, and signaling responses generated by MD and provided the molecular insight into the integration of cell homeostasis and metabolic controls in fish species.

Keywords: Methionine deprivation; Turbot (*Scophthalmus maximus* L.); Nutrient sensing; Amino acids; Metabolism

1. Introduction

Methionine is one of the most limited essential amino acids in plant protein sources [1,2]. Methionine deficiency is correlated with reductions of weight gain, feed conversion efficiency, and nitrogen retention in chicks [3–5], pigs [6–10] and fish [11–14]. This becomes more of a challenge than ever before because of increased inclusion of plant proteins in animal feeds [15]. As the primary methyl and aminopropyl donors for a variety of molecules, methionine and its metabolites are critical for homeostasis maintenance [16–19]. Better understanding the cellular signaling and metabolic regulation associated with methionine is critical for a better design of efficient nutritional strategies, especially for fish, whose metabolism is much less studied than that in mammals.

Animals respond to nutrient availability through sophisticated interplays between cellular signaling pathways and coordinated metabolic processes [20–24]. Intracellular sensing of amino acid concentrations is mediated at least by two distinct, yet complementary pathways, the target of rapamycin (TOR) signaling and the amino acid response (AAR) pathways [25]. Amino acids, especially leucine, activate TOR signaling pathway [26], which leads to the phosphorylation of ribosomal protein S6 kinase 1 (S6 K1) and eukaryotic initiation factor 4E binding protein-1 (4E–BP1), and induction of protein synthesis [27]. Deficiency of dietary protein or imbalance of essential amino acids generally activates AAR signaling pathway, through which general controlled nonderepressible 2 (GCN2) kinase detects uncharged tRNA and phosphorylates eukaryotic translation initiation factor (eIF2α) [28]. This triggers global protein synthesis suppression and induces translation of rate limiting enzymes related to metabolism [29,30]. Thus, based on the nutrient availability, nutrient sensing pathways either engage in anabolism and storage, or trigger homeostatic mobilization of internal stores for catabolism [29,30]. These regulatory signaling networks have been demonstrated to be vital in response to dietary protein sources [31,32], protein levels [33], amino acids [34,35], and anti-nutritional factors [36] in fish.

Omics technologies allow a global and in-depth characterization of the physiological reactions produced by stimuli [37]. In particular, proteomics has the advantage of measuring protein and its modifications [38], enabling the modeling of biological processes, as well as the elucidation of novel biomarkers that are sensitive to nutritional interventions [39]. Proteomics has been demonstrated as a powerful tool to globally evaluate the effects of dietary formulations on tissues and/or whole carcass in fish species [40–43].

☆ Conflict of Interest: None

☆☆ Sources of Funding: This study was supported by National Natural Science Foundation to G.H. (31572627), 973 program to K.M. (2014CB138602), and Aoshan Scholarship to G.H. by Qingdao National Laboratory for Marine Science and Technology.

* Corresponding author. Tel.: +86 532 82031589; fax: +86 532 82031627.
E-mail address: hegen@ouc.edu.cn (G. He).

http://dx.doi.org/10.1016/j.jnutbio.2017.08.015
0955-2863/

To date, most of the studies on the evaluation of a particular nutrient in fish have counted on the post analyses after feeding trial [33,34,44]. The results are greatly influenced by feeding environments [45], animal health [46], diet palatability [47] and digestibility [48]. All these factors significantly obscure the response generated by the target nutrient and make it hard to compare among studies. Only a limited number of nutritional studies were conducted on fish cell lines [36,49,50], with few on the characterization of the nutrient sensing and metabolic networks.

In the present study, we hypothesized that methionine deprivation (MD) would substantially influence the TOR and AAR signaling and downstream metabolic pathways, as well as the global homeostasis in fish cells. To test this hypothesis, we took the initial steps to establish primary muscle cells of turbot (*Scophthalmus maximus*). Using the turbot primary muscle cells, we employed an approach that combined the activity measurements of nutrient sensing pathways with an isobaric tag for relative and absolute quantitation (iTRAQ)-based proteomic analysis of differentially expressed proteins, as well as quantitation of mRNA expressions of key signaling and metabolic molecules after MD. Such multi-level characterizations should provide clear interlinks among metabolic reactions and better mechanistic understanding than before.

2. Materials and methods

2.1. Generation of turbot primary muscle cells

The primary cell culture was generated as described before [51]. Turbot weighed approximately 10 g was sacrificed and immersed in 75% alcohol for 30 s, and then rinsed by sterilized Dulbecco's phosphate-buffered saline (DPBS) with 400 units ml^{-1} penicillin and 400 μg ml^{-1} streptomycin. White dorsal muscle was excised and collected in cold (4°C) Leibowitz's L-15 Medium (Sigma: L5520). The tissue was then cut into 1.0 mm^3 pieces using sterilized stainless-steel scissors and forceps. The tissue pieces were centrifuged (300×*g*, 1 min) to collect the pellet and then resuspended in 5 ml L-15 medium. This operation was repeated for three times and then the pellet was resuspended in 0.1% trypsin in L-15 medium. Enzymatic digestion was performed for 10 min at 21°C with gentle agitation and centrifuged for 1 min at 300 g. The supernatant was diluted with 2 volumes of cold L-15 medium with 20% serum to block trypsin activity. The tissue fragments were subjected to a second trypsin digestion. The supernatants were pooled, filtered through a 100-μm nylon cell strainer and centrifuged (300×*g*, 20 min, 4°C). The pellet was resuspended in growth medium (L-15 medium with 20% serum and 2.5 ng/ml fibroblast growth factor) and diluted to reach a final concentration of 2×10^6 cells/ml and cultured at 24°C in a humidified incubator without CO_2.

2.2. Cell treatment

Turbot primary muscle cells were cultured in growth medium. When reached 90% confluency, cells were rinsed by DPBS twice and then changed to L-15 medium with (CON) or without (MD) methionine in the presence of 1% insulin (Gibco: 41,400,045) for 12 h. Treated cells were collected for ITRAQ-based proteomics (Fig. S1), western blotting, and quantitative real-time PCR.

2.3. ITRAQ-based proteomics analyses

The detailed experimental procedure for iTRAQ-based proteomic analyses was conducted as described before [52]. Cells were scraped and extracted with 100 mM Tris, 4% SDS, 1 mM DTT, pH 7.6. Total proteins were subjected to trypsin digestion, iTRAQ labeling, strong cation exchange (SCX) chromatography, high-performance liquid chromatography (HPLC), and analyzed by the electrospray ionization tandem mass spectrometry (ESI MS/MS) (Q-Exactive, ThermoFinnigan, San Jose, CA, USA). For the MALDI-TOF-MS/MS, total proteins were digested with trypsin and subjected to the MALDI-TOF MS/MS (4800 Plus MALDI TOF/TOFTM Analyzer, Applied Biosystems, USA).

2.4. Quantitative real-time PCR (qRT-PCR)

For qRT-PCR, cells were lysed with Trizol reagent (Invitrogen, USA) according to the manufacturer's instruction. The extracted RNA was quantified by a Nanodrop 2000 spectrophotometer (Thermo) and the integrity was examined by 1.5% denatured agarose gel electrophoresis. The qRT-PCR was conducted as described previously [53]. Primer sequences for qRT-PCR were listed in Table S1. To calculate the expression levels of target genes, results were normalized to reference gene RNA polymerase II subunit D (RPSD), as no expression changes of RPSD were observed between treatments. The expression levels of target genes were quantitated by the $2^{-\Delta\Delta Ct}$ method [54]. Gene expression levels were reported as fold of CON.

2.5. Western blot analyses

For Western blot analyses, cells were rinsed twice with ice-cold DPBS and lysed in ice-cold lysis buffer composed of 50 mM Tris, 150 mM NaCl, 0.5% NP-40, 0.1% SDS, 1 mM EDTA, pH 7.4, with protease and phosphatase inhibitor cocktail (Roche). The supernatant was collected after centrifugation at 12,000×*g* for 20 min at 4°C. Protein concentrations were determined by a BCA protein assay kit (Beyotime Biotechnology) according to the manufacturer's instructions. After normalization, samples were separated by SDS-PAGE and transferred to 0.45 μm PVDF membrane (Millipore). The membrane was blocked with 5% nonfat dry milk in TBST for 1 h and incubated with primary antibodies overnight, followed by secondary antibodies for 1 h, and developed with Beyo ECL Plus reagents (Beyotime). The following antibodies were used: antibodies against phospho-ribosomal protein S6 (Ser235/236) (Cat. no. 4856), S6 (Cat. no. 2217), phospho-4E-BP1 (Thr37/46) (Cat. no. 9459), 4E–BP1 (Cat. no. 9452), phospho-AMPK (Thr172) (Cat. no. 2531), AMPK (Cat. no. 5831), phospho- S6 K (Thr421/Ser424) (Cat. no. 9204), S6 K (Cat. no. 9202), eIF2α (Cat. no. 9722), phospho-eIF2α (Ser51) (Cat. no. 3597), β-tubulin (Cat. no. 2146) were purchased from Cell Signaling Technology Inc. Activating transcription factor 4 (ATF4) (Cat. no. sc-200) were purchased from Santa Cruz Biotechnology Inc. All antibodies was verified and successfully used in turbot as reported before [31,32,36,55]. All experiments were repeated at least 3 times. The densities of the protein bands were normalized to that of β-tubulin, which served as an inner control. All the band intensities were quantified using NIH Image 1.63 software. The data were expressed as mean±S.E.M.

2.6. Determination of cellular nascent protein synthesis

The nascent protein synthesis was measured by a ClickiT Plus OPP Alexa Fluor 488 Protein Synthesis Assay Kit (Life Technologies, Grand Allen, TX, USA) as reported before [56] following the manufacturer's instructions. Specifically, turbot primary muscle cells were plated at a density of 2.5×10^5 cells/mL into 96-well plates containing 100 μl of L-15 complete medium. After 24 h incubation, cells were replaced with CON and MD medium for 12 h. Cells were then incubated with 20 mM Click-iT1 OPP working solution for 30 min, fixed with 4% paraformaldehyde in PBS, and then permeabilized with 0.5% Triton X-100 in PBS. Cells were then incubated with Click-iT1 Plus OPP reaction cocktail for 30 min at room temperature, protected from light, and incubated with NuclearMask™ to label nuclei. Images were taken by a fluorescence microscopy (Eclipse Ti-s, Nikon, Japan). Nascent protein synthesis was quantitated by regions of interest (ROIs) statistics in NIS-Elements 4.0 to calculate signal intensity in the green fluorescent channel in the ring around the nucleus [57].

2.7. Measurement of intracellular free amino acids

The concentrations of intracellular free amino acids were measured based on the methods described before [58,59] with some modifications. Briefly, after MD treatment, cells were rapidly washed with 10 ml of cold DPBS twice and chilled with 2 ml cold methanol on dry ice. Cells were collected with a rubber tipped cell scraper and transferred to 15-ml conical tubes. The dishes were washed two times with 1 ml methanol and the sample was transferred to liquid nitrogen for 10 min, thawed in an ice bath for 10 min, and briefly vortexed. This freeze–thaw cycle was repeated three times for complete cell disruption. The sample was centrifuged at 4°C and 3000×*g* for 30 min and the supernatant was transferred to a new tube. The pellet was lysed in 1 ml of lysis buffer (50 mM Tris, 150 mM NaCl, 0.5% NP-40, 0.1% SDS, 1 mM EDTA, pH 7.4, with protease inhibitor cocktail) and the protein concentration was quantitated using a BCA Protein Assay kit (Beyotime Biotechnology) according to the manufacturer's instructions. After sample normalization based on total protein levels, supernatants were de-proteinized by mixing with equal volume of 10% sulfosalicylic acid and incubated at 4 ° C for 5 min. After centrifugation at 13000 rpm for 15 min, 1 ml of supernatant was filtered through 0.22-μm filters for free amino acid measurement using an automatic amino acid analyzer (L-8900, HITACHI, Japan).

2.8. Free fatty acid measurement

The intracellular free fatty acid content was measured according to the previous reports [60]. The free fatty acids were extracted from approximately 10^6 cells with 200 μl of chloroform-Triton X-100 (1% Triton X-100 in pure chloroform) using Dounce homogenizer. After centrifugation at 13000×*g* for 10 min, the organic phase (lower phase) was collected and vacuum dried. Free fatty acid was measured using a free fatty acid kit (Cat. no. K612–100 BioVision) following the manufacturer's instructions and measured at 570 nm using a SpectraMax i3x multi-mode detection platform (Molecular Devices, USA).

2.9. Analysis of oxygen consumption rate

The intracellular oxygen consumption was measured using an oxygen consumption rate kit (Cat. no. 600800, Cayman) as described before [61]. Specifically, after MD treatment, cells in 96-well plates were replaced with medium containing the MitoXpress probe, and covered with 100 μl mineral oil to seal off the air supply. The fluorescence intensity was measured at Ex. 380 nm and Em. 650 nm every 30 s for 60 min at 25 °C using a SpectraMax i3x multi-mode detection platform (Molecular Devices, USA). Oxygen consumption rates were determined by calculating the slope of the linear regions of the oxygen consumption curves using GraphPad Prism 6 software.

2.10. Statistical analysis

Each value is expressed as means±S.E.M. All statistical evaluations were analyzed by independent *t* tests using the software SPSS 22.0.0.0. A value of $P<.05$ was considered statistically significant.

3. Results

3.1. Changes of intracellular homeostasis after MD

During the experimental period (12 h), the cell viability was not influenced (Fig. S2). After 12 h MD, the intracellular free methionine level was too low to detect (< 20 pM) in MD group, while the intracellular free methionine level in CON group was 1.04±0.32 μM (Fig. 1A). However, the intracellular concentrations of other amino acids were increased between 146–355% (Fig. 1A). On the other hand, cellular protein synthesis rate was dropped by 24.49±2.61% in MD compared to control (Fig. 1B and C; $P<.05$). The intracellular free fatty acid levels were also reduced by 12.17±2.23% in MD group (Fig. 1D; $P<.05$). Furthermore, the cellular oxygen consumption rate was increased by 37.08±5.93% in MD group (Fig. 1E and F).

3.2. Changes of nutrient sensing pathways after MD

The activity of nutrient sensing TOR signaling pathway, represented by the phosphorylation levels of S6 K (Thr^{421}/Ser^{424}), S6 ($Ser^{235/236}$) and 4E–BP1 ($Thr^{37/46}$), was decreased after MD treatment (Fig. 2A; $P<.05$). On the contrary, the activity of AAR pathway, represented by the levels of phospho-eIF2α and ATF4, was increased by MD (Fig. 2A; $P<.05$). This was further confirmed by the significant increases of mRNA expressions of major AAR molecules [29], including *gcn2*, asparagine synthetase (*asns*), *atf4* and C/EBP homology protein (*chop*) after 12 h MD treatment (Table 1; $P<.05$). The expressions of *sestrin1* and *2*, which were AAR effectors and TOR suppressors [62], were up-regulated by MD (Table 1; $P<.05$). The activity of energy sensing AMPK, represented by its phosphorylation, was increased by MD (Fig. 2A; $P<.05$). The mRNA expression of a key mediator of energy expenditure, uncoupling protein 1 (*ucp1*), was also increased (Table 1; $P<.05$).

3.3. Overview of the iTRAQ-based proteomic analyses

Using LC–MS/MS analyses, a total of 6288 proteins were quantified and compared between the CON and the MD groups. 379 proteins were

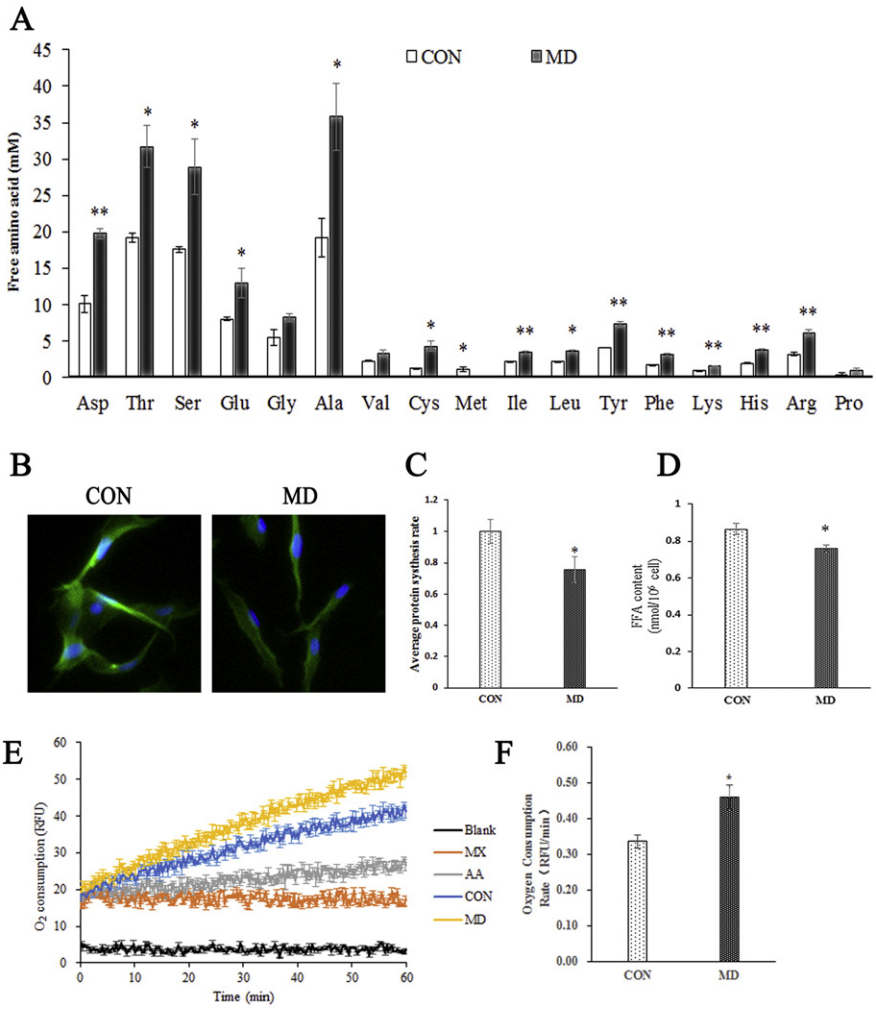

Fig. 1. MD influenced cellular homeostasis. (A) Intracellular free amino acids concentration changes after MD. (B) Representative images from the experiment to measure protein synthesis. (C) Approximately 300 total cells were automatically quantified for fluorescence intensity corresponding to protein synthesis rate. The data were presented as bar graphs normalized to CON group. (D) Intracellular free fatty acid content changes after MD. (E) The MitoXpress® Xtra-Oxygen Consumption Assay was used to monitor oxygen consumption *via* fluorescence generation. Blank, empty wells with medium; MX, empty wells with medium and MitoXpress probe; AA, cells in full medium with antimycin A and MitoXpress probe; CON, cells in CON medium with MitoXpress probe; MD, cells in MD medium with MitoXpress probe. (F) Oxygen consumption rate in CON and MD group were calculated by measuring the slopes of the linear regions of the oxygen consumption curves. Results were represented as means with standard errors ($n=3$) and were analyzed using independent *t* tests. $^{*}P<.05$, $^{**}P<.01$.

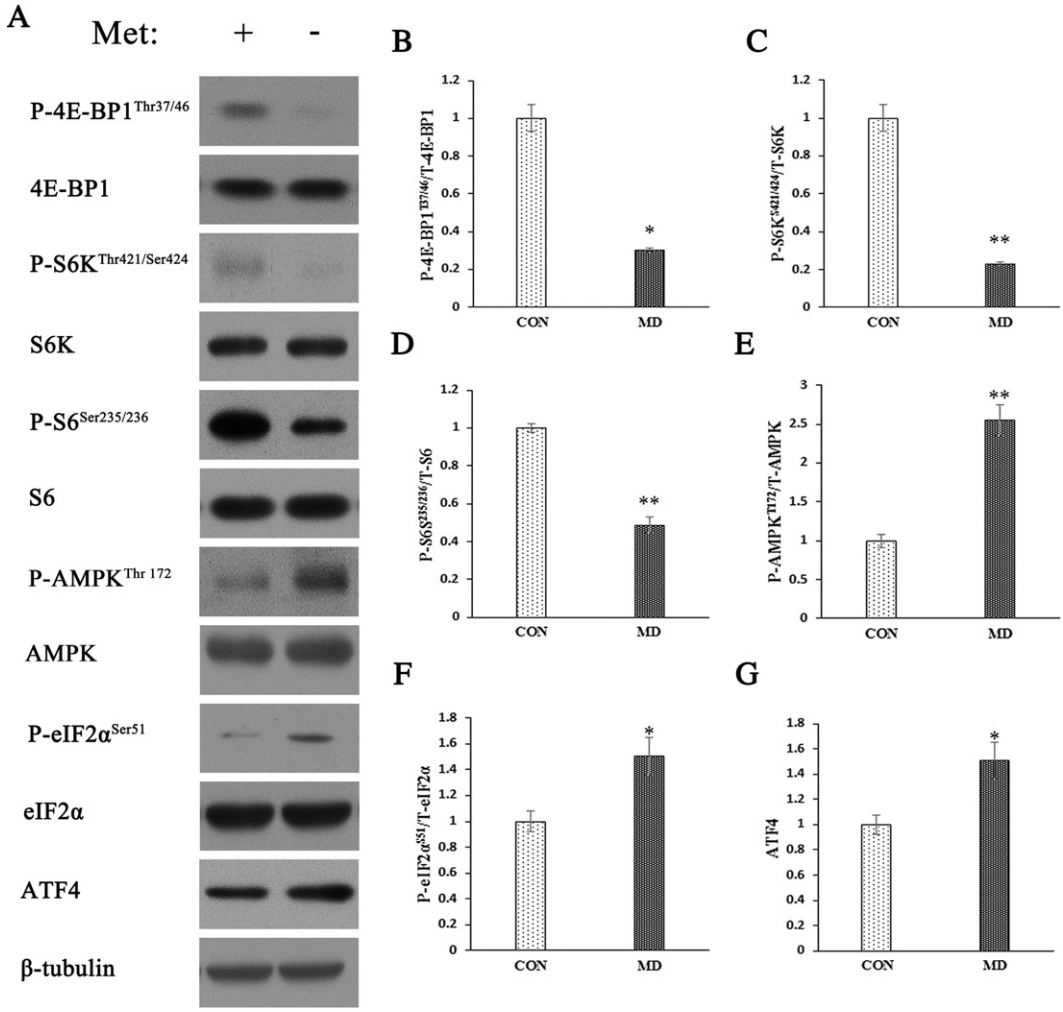

Fig. 2. Nutrient sensing signaling changes under MD. The levels and/or phosphorylations of 4E–BP1, S6 K, S6, eIF2α,AMPK, and ATF4 were examined by western blots (A) and quantitated (B-G). Results are represented as means with standard errors (n=3) and were analyzed using independent t tests. *P<.05, **P<.01.

identified as differentially expressed proteins with significance (P<.05, Supplementary document 2). Functional annotations of these proteins were further performed based on gene ontology (GO). The differentially expressed proteins were mainly localized in membranes, organelles, and macromolecular complexes (Fig. 3). They were engaged in metabolic processes, biological regulations, and associated with biological functions like binding and catalytic activities (Fig. 3). Using Fisher's exact test, 22 KEGG pathways were identified to be significantly influenced (Table S2; P<.05), 9 of which were associated with nutritional metabolism (Table 2; P<.05). These included various biological processes, such as amino acid metabolism, fatty acid metabolism and energy metabolism.

Table 1
Relative mRNA expressions of genes involved in nutrient sensing pathways in turbot primary muscle cells treated with MD for 12 h[1]

Gene	Fold of CON		
	CON	MD	P-value
gcn2	1.00±0.03	1.65±0.14	0.005
atf4	1.00±0.02	1.33±0.06	0.003
asns	1.00±0.03	2.35±0.10	<0.001
chop	1.00±0.02	1.65±0.05	<0.001
snat2	1.00±0.06	1.25±0.03	0.013
sesn1	1.01±0.05	2.94±0.06	<0.001
sesn2	1.00±0.04	1.26±0.04	0.001
ucp1	1.01±0.06	2.05±0.13	<0.001

[1] The data are expressed as means±S.E.M. (n=6). The differences between experimental groups were tested using independent t tests. *gcn2*, general control nonderepressible 2; *atf4*, activating transcription factor 4; *asns*, asparagine synthetase; *chop*, C/EBP homology protein; *snat2*, sodium-coupled neutral amino acid transporter 2;*sesn1*, sestrin 1; *sesn2*, sestrin 2;*ucp1*,uncoupling protein 1.

3.4. MD induced amino acid catabolism

Cellular amino acid metabolic process was identified as the most influenced biological process based on the gene ontology (GO) enrichment (Supplement Fig. S3, 4). Several KEGG pathways such as "biosynthesis of amino acids", "valine, leucine and isoleucine degradation", and "lysine degradation" were significantly altered (Table 2; P<.05). Two lysosomal proteases, carboxypeptidase C and cathepsin D, were increased in MD group (Table 3). Key enzymes in amino acid catabolism including glutamate dehydrogenase (GLUD1), agmatinase, omega-amidase, L-serine ammonia-lyase (SDS), and methylmalonyl-CoA/ethylmalonyl-CoA epimerase were up regulated. The LC–MS/MS data were further validated by real-time quantitative PCR. The mRNA expression of the E3 ubiquitin ligase, muscle RING finger 1 (*murf1*), was increased by MD (Table 4; P<.05). The mRNA levels of *glud1*, *sds* and branch-chain α-keto acid dehydrogenase E2 subunit (*bckdh-e2*) were also significantly increased (Table 4; P<.05). On the contrary, the amino acid

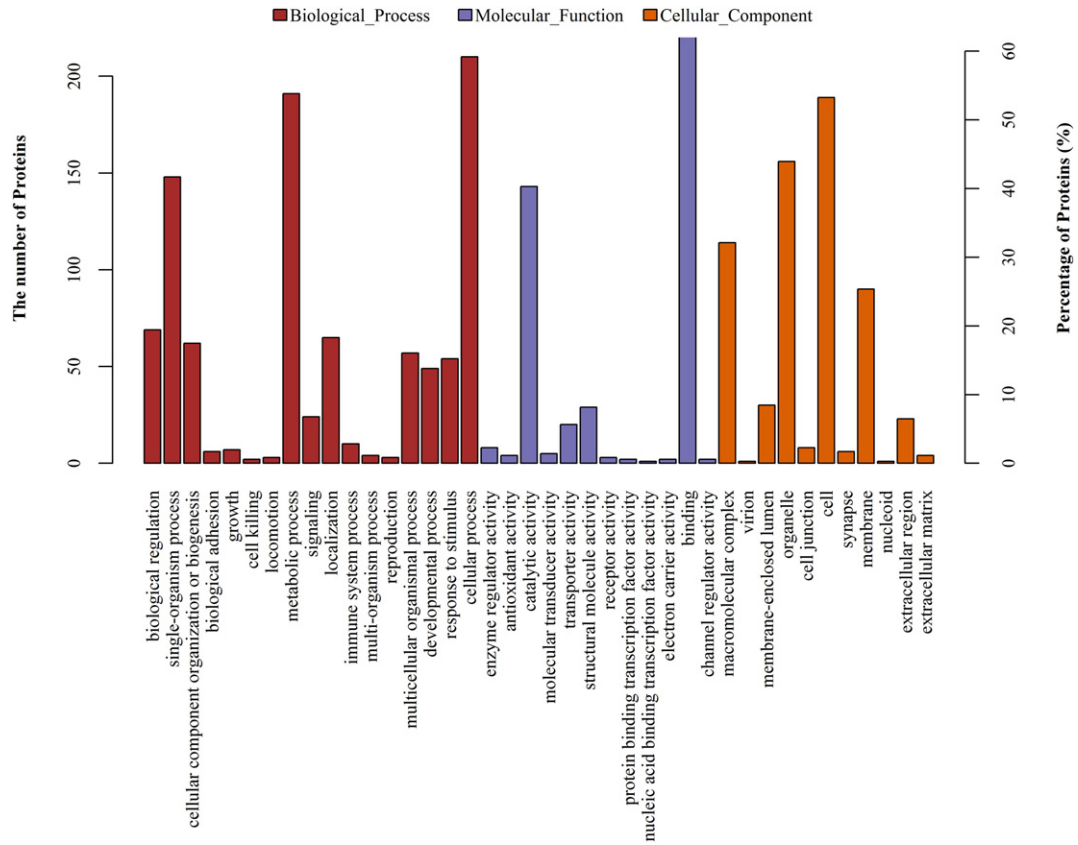

Fig. 3. Gene Ontology classifications of proteins differentially expressed between CON and MD treated turbot muscle cells for 12 h. The differentially expressed proteins were grouped into three hierarchically structured GO terms: biological process, cellular component and molecular function.

anabolic D-3-phosphoglycerate dehydrogenase (PHGDH) and glutamine synthetase (GS) were down regulated (Table 3; $P<.05$).

3.5. MD induced fatty acid catabolism

The KEGG analysis showed that "fatty acid degradation" was significantly influenced by MD (Table 2; $P<.05$). Protein levels of key enzymes in β-oxidation, including carnitine o-palmitoyltransferase (CPT) 2 [63], acyl-CoA dehydrogenase (ACAD), enoyl-CoA hydratase (ECHA), and 3-hydroxyacyl-CoA dehydrogenase (HADH) [64] were increased after MD treatment (Table 3; $P<.05$).

To validate our proteomic results, the mRNA expressions of key enzymes in fatty acid metabolism were also quantitated (Table 4; $P<.05$). The expressions of genes involved in fatty acid (FA) synthesis, including fatty acid synthetase (*fas*) and glucose-6-phosphate dehydrogenase (*g6pd*) [33] were down regulated in MD group. The expressions of genes involved in β-oxidation [65] including acyl-CoA oxidase 1 (*acox1*), *cpt1a*, *hadh*, as well as nuclear receptors involved in FA catabolism including peroxisome proliferator activated receptor alpha 1 (*pparα1*), peroxisome proliferator activated receptor alpha 2 (*pparα2*) and peroxisome proliferator activated receptor beta (*pparβ*), were up regulated in MD group.

Table 2
Enriched KEGG pathways on nutritional metabolism with significance

	Map Name	Map ID	count	*P* value
1	Citrate cycle (TCA cycle)	ko00020	8	0.022
2	Oxidative phosphorylation	ko00190	20	<0.001
3	Fatty acid degradation	ko00071	6	0.032
4	Valine, leucine and isoleucine degradation	ko00280	8	0.027
5	Biosynthesis of amino acids	ko01230	11	0.048
6	Lysine degradation	ko00310	6	0.020
7	Carbon metabolism	ko01200	20	0.005
8	Protein digestion and absorption	ko04974	8	0.007
9	Non-alcoholic fatty liver disease (NAFLD)	ko04932	16	<0.001

3.6. MD inhibited glycolysis and enhanced energy metabolism

MD reduced key enzymes in glycolysis at protein level. These included enolase (ENO), glucose-6-phosphate isomerase (GPI), glyceraldehyde 3-phosphate dehydrogenase (GAPDH), phosphoglycerate kinase (PGK) and pyruvate kinase (PK) (Table 3; $P<.05$). Consistent with the proteomic data, the mRNA levels of glucokinase (*gk*) and *pk* were also down regulated (Table 4; $P<.05$). A positive transcription regulator of glycolysis, hypoxia-inducible factor 1-alpha (*hif1α*) [30], was also down regulated (Table 4; $P<.05$).

MD increased key enzyme levels of TCA cycle. These included citrate synthase (CS), isocitrate dehydrogenase (NAD+) (IDH) and dihydro lipoamide acetyl transferase (DLAT) (Table 3; $P<.05$) [66]. The levels of key molecules involved in oxidative phosphorylation were also increased. These included ubiquinol-cytochrome c reductase, NADH dehydrogenase, cytochrome c oxidase cbb3-type subunit I, and F-type H^+-transporting ATPase subunits (Table 3; $P<.05$). These results were further confirmed at transcription level. The mRNA expressions of *cs*, *idh*1, dihydro lipoamide succinyl transferase (*dlst*), F-type H^+-transporting ATPase subunit alpha (*Atp5α*), and F-type H^+-transporting ATPase subunit epsilon (*atp5ε*) were up regulated in MD group (Table 4; $P<.05$).

4. Discussion

In the present study, to ensure the specificity of the results, we selected a MD condition that during the experimental period (12 h),

Table 3
Differentially regulated proteins related to amino acid metabolism, fatty acid metabolism and energy metabolism identified by iTRAQ in turbot primary muscle cells treated with MD for 12 h

Accession no.	name	MD/CON ratio (mean±S.E.)	Expression pattern	*P*-value of ratio	Coverage	Proteins	Unique Peptides
Protein degradation							
H2M553	Carboxypeptidase C	1.21±0.02	↑	0.021	2.58	1	1
H2M553	Cathepsin D	1.20±0.01	↑	0.038	4.51	1	1
Amino acid degradation							
G1FKH1	Glutamate dehydrogenase (NAD(P)+)	1.26±0.01	↑	0.008	42.86	1	1
G3PAM8	Agmatinase	1.31±0.01	↑	0.002	2.92	2	1
F6KMH3	Omega-amidase	1.23±0.16	↑	0.017	5.56	11	1
A0A087XY05	L-serine ammonia-lyase	1.25±0.06	↑	0.007	5.9	2	1
H3C428	Methylmalonyl-CoA/ethylmalonyl-CoA epimerase	1.27±0.02	↑	0.007	6.99	7	1
Amino acid synthesis							
H2BL58	Glutamine synthetase	0.78±0.10	↓	0.002	9.43	32	1
I3JQ92	D-3-phosphoglycerate dehydrogenase	0.80±0.01	↓	0.007	9.03	3	4
Fatty acid degradation							
G3NIA5	Carnitine O-palmitoyltransferase 2	1.32±0.01	↑	0.002	4.4	8	3
Q4SUC5	Acyl-CoA dehydrogenase	1.24±0.02	↑	0.013	2.35	6	1
I3IXE6	Enoyl-CoA hydratase	1.23±0.01	↑	0.021	13.2	2	2
G3PZP2	3-hydroxyacyl-CoA dehydrogenase	1.39±0.02	↑	0.000	6.14	7	1
I3K6X0	Long-chain-acyl-CoA dehydrogenase	1.21±0.01	↑	0.034	2.71	1	1
I3KQN0	Aldehyde dehydrogenase (NAD+)	1.29±0.00	↑	0.003	2.88	1	1
Glycolysis							
G3NX35	enolase	0.69±0.00	↓	0.000	47.22	36	1
Q8QFT2	Glucose-6-phosphate isomerase	0.83±0.04	↓	0.025	12.12	14	1
Q27ID6	Glyceraldehyde 3-phosphate dehydrogenase	0.77±0.02	↓	0.001	40.67	10	3
A0A087X2K2	Phosphoglycerate kinase	0.77±0.04	↓	0.001	19.18	4	1
G3NT93	Pyruvate kinase	0.81±0.08	↓	0.008	17.55	7	1
Citrate cycle (TCA cycle)							
A0A096M7D3	Dihydrolipoamide acetyltransferase	1.21±0.02	↑	0.034	17.55	7	1
Q6S9V6	Citrate synthase	1.21±0.05	↑	0.034	21.32	9	2
M4ASL2	isocitrate dehydrogenase (NAD+)	1.29±0.01	↑	0.004	10.84	6	2
H2SRU2	Succinyl-CoA synthetase alpha subunit	1.30±0.00	↑	0.003	13.26	7	2
Oxidative phosphorylation							
F1C745	Ubiquinol-cytochrome c Reductase core subunit 1	1.24±0.03	↑	0.014	16.74	2	1
C3KIB4	Ubiquinol-cytochrome c Reductase subunit 9	1.25±0.01	↑	0.010	12.9	2	1
C3KIN3	NADH dehydrogenase	1.28±0.01	↑	0.006	6.3	8	1
C7S7A9	Cytochrome c oxidase cbb3-type subunit I	1.25±0.00	↑	0.012	11.3	461	1
Q4S7Z7	F-type H^+-transporting ATPase subunit epsilon	1.28±0.00	↑	0.005	43.9	3	2
I3J6Z6	F-type H^+-transporting ATPase subunit e	1.29±0.01	↑	0.004	33.8	3	1
H2TPW6	F-type H^+-transporting ATPase subunit gamma	1.20±0.03	↑	0.038	13.31	12	4
H2MW66	F-type H^+-transporting ATPase subunit d	1.30±0.01	↑	0.003	6.93	3	1
C7S7B1	F-type H^+-transporting ATPase subunit a	1.23±0.02	↑	0.019	5.63	2	1
C3KHM0	F-type H^+-transporting ATPase subunit g	1.22±0.05	↑	0.027	12.62	4	1
G3NTD6	F-type H^+-transporting ATPase subunit alpha	1.28±0.03	↑	0.005	33.76	2	3

the cell viability was not influenced (Fig. S2). However, 12 h MD already disrupted cellular homeostasis. Nascent protein synthesis was significantly reduced, which in turn caused the accumulation of other free amino acids except methionine. The intracellular lipid pool was also partially depleted (Fig. 1D). Increased cellular oxygen consumption (Fig. 1F) suggested elevated cellular energy expenditure. These results were consistent with and underlay the common phenotypes of reduced body protein and lipid content by low methionine diet in fish species [44,67,68]. A comprehensive characterization of molecular responses of nutrient sensing and metabolic pathways, as discussed below, should provide an in-depth understanding of these phenotypic consequences.

The presence of amino acids is sensed through TOR signaling pathway [20], while the AAR signaling is triggered by interactions between GCN2 and uncharged cognate tRNA, which becomes available after amino acid deficiency [69]. AAR activation would also sustain TOR suppression upon amino acid deprivation [62]. Our results demonstrated that MD inhibited TOR signaling, evidenced by reduced phosphorylation of S6 K, S6 and 4E–BP1 (Fig. 2). On the other hand, the expressions of major AAR signaling molecules (*gcn2*, *asns*, phospho-eIF2α,*atf4* and *chop*) were increased (Fig. 2, Table 1), suggesting a stimulated AAR pathway, consistent with previous observations in cancer cell lines after MD [29], or dietary methionine deficiency in rainbow trout [70]. Furthermore, the expression of *sestrin 2*, an effector of AAR and negative regulator of TOR [71], was also increased under MD (Table 1). Mechanistically, the activated AAR and inhibited TOR signaling pathway would reduce protein synthesis [25,72], which was confirmed in the present study (Fig. 1B and C). We also observed that AMPK, a critical cellular energy sensor [73,74], was activated under MD. S-adenosylmethionine (SAMe), a metabolite of methionine [18], was known to inhibit the phosphorylation of AMPK [75]. Decreased SAMe under MD would contribute to AMPK activation [76]. On the other hand, increased sestrins, as mentioned above, could also function as an AMPK activator (Table 1) [77]. Modulation of AMPK activities would lead to significant changes of energy metabolism, which is discussed below.

The comparative proteomic analyses provided a clear global picture on the changes of metabolic processes under MD. Carboxypeptidase C and cathepsin D are major lysosomal proteases [78], while murf1 is a key molecule responsible for proteosomal muscle protein degradation [79]. The increased levels of all these enzymes (Tables 3, 4) suggested up regulation of protein degradations under MD. The KEGG analysis suggested that MD significantly influenced the degradation of multiple amino acids including valine, leucine, isoleucine and lysine. Specifically, levels of key enzymes responsible for amino acid degradation (GLUD1, SDS, and BCKDH) were up regulated, while those for amino acid synthesis (PHGDH and GS) were down regulated.

KEGG analysis indicated that MD influenced fatty acid degradation (Table 2). Specifically, the levels of major lipid degradation enzymes were increased while those for lipid synthesis were decreased at both

Table 4
Relative mRNA expressions of genes involved in amino acid degradation, FA metabolism, glycolysis and energy metabolism in turbot primary muscle cells treated with MD for 12 h[1]

Gene	Fold of CON		
	CON	MD	*P*-value
Protein degradation			
murf1	1.00±0.11	2.03±0.24	0.003
Amino acid degradation			
sds	1.00±0.06	1.20±0.03	0.022
glud1	1.00±0.04	1.16±0.04	0.022
bckdh-e2	1.00±0.06	1.92±0.20	0.001
Fatty acid metabolism			
Fatty acid synthesis			
fas	1.00±0.05	0.71±0.07	0.017
srebp1	1.00±0.04	0.84±0.03	0.029
g6pd	1.00±0.03	0.74±0.02	<0.001
Fatty acid β-oxidation			
acox1	1.00±0.05	1.27±0.11	0.048
cpt1a	1.00±0.06	1.32±0.08	0.014
hadh	1.00±0.03	1.22±0.03	0.001
Nuclear receptors involved in Fatty acid metabolism			
pparα1	1.00±0.08	1.73±0.17	0.007
pparα2	1.00±0.04	1.38±0.07	0.001
pparβ	1.00±0.07	1.96±0.11	<0.001
Glycolysis			
gk	1.00±0.05	0.66±0.03	0.001
pk	1.00±0.06	0.84±0.02	0.030
hif1α	1.00±0.03	0.74±0.04	0.045
Energy metabolism			
TCA cycle			
cs	1.00±0.03	1.12±0.04	0.033
idh1	1.00±0.03	1.19±0.04	0.004
dlst	1.00±0.03	1.32±0.04	<0.001
oxidative phosphorylation			
atp5α	1.00±0.04	1.23±0.05	0.006
atp5ε	1.00±0.02	1.13±0.03	0.003

[1] The data are expressed as means±S.E.M. (n=6). The differences between experimental groups were tested using independent t tests. *murf1*, muscle RING-finger 1; *sds*, L-serine or L-threonine ammonia-lyase; *glud1*, glutamate dehydrogenase 1; *bckdh-e2*, branch-chain α-keto acid dehydrogenase E2 subunit; *fas*, fatty acid synthetase; *srebp1*, sterol regulatory element-binding protein 1; *g6pd*, glucose-6-phosphate dehydrogenase; *acox1*, acyl-CoA oxidase 1; *cpt1a*, carnitine palmitoyltransferase 1 isoforms A; *hadh*, 3-hydroxyacyl-CoA dehydrogenase; *pparα1*, peroxisome proliferator activated receptor alpha 1; *pparα2*, peroxisome proliferator activated receptor alpha 2; *pparβ*, peroxisome proliferator activated receptor beta; *gk*, glucokinase; *pk*, pyruvate kinase; *hif1α*, hypoxia-inducible factor 1-alpha; *cs*, citrate synthesis; IDH1, isocitrate dehydrogenase1; *dlst*, dihydrolipoamide succinyltransferase; *atp5α*, F-type H^+-transporting ATPase subunit alpha; *atp5ε*, F-type H^+-transporting ATPase subunit epsilon.

mRNA (Table 4) and protein levels (Table 3). Similarly, lipogenesis was suppressed in mice upon leucine deprivation [80]. Activation of lipogenic genes requires the sterol response element binding protein (SREBP) transcription factors, which could be inducted by TOR signaling [30]. As discussed above, TOR activity was reduced while the expression level of *srebp1* was down regulated under MD (Table 4). GCN2 was also reported to be involved in the regulation of lipogenesis upon amino acid deprivation [80].

The levels of major enzymes in glycolysis, including ENO, GPI, GAPDH, PGK and PK (Tables 3, 4), were all reduced, suggesting the suppression of this process under MD. Reduced glycolysis was also suggested in rainbow trout fed with methionine deficiency diet [44]. In most cells, glycolysis is not the major ATP contributor. Rather, a major function of glycolysis is to provide intermediates for anabolic biosynthesis [81]. Thus, reduced glycolysis was synchronized with suppression of anabolism under MD. Such coordination was mediated though the regulation of TOR activities and its downstream effectors such as *hif1a*, which acted upstream of glycolysis [30] and was also down regulated by MD.

KEGG analysis showed that MD significantly influenced TCA cycle and oxidative phosphorylation (Table 2), which was the major energy producer in cells. Both mRNA and protein levels of key enzymes of TCA cycle and oxidative phosphorylation were increased (Tables 3, 4), suggesting stimulated energy expenditure. This was further confirmed by the increased oxygen consumption rate in MD group (Fig. 1F). Consistently, MD activated AMPK signaling, which enhanced FA oxidation for ATP production [73,74]. Uncoupling protein 1 (UCP1) is a key mediator for energy expenditure and associated with AMPK activation [82–84]. In the present study, the *ucp1* level was also up regulated (Table 4). This was consistent with what was reported in rat fed methionine restriction diet [85]. As discussed above, stimulated amino acid and fatty acid degradations should provide increased fluxes of metabolic intermediates (pyruvic acid, alpha-ketoglutarate, acetyl-CoA) for TCA cycle and oxidative phosphorylation.

In conclusion, this study provided a comprehensive characterization on how MD was detected and how sensing of the deprivation was translated into highly integrated transcriptional, proteomic, and metabolic responses in turbot primary muscle cells. First, inhibition of TOR and activation of AAR signaling by MD led to reduced protein synthesis. Second, MD triggered degradation of multiple amino acids, highlighting the tight regulation of amino acid balance by cells. Third, reduced glycolysis and lipogenesis, as well as increased lipolysis by MD demonstrated the close metabolic connections among macronutrients. Increased catabolism and energy expenditure under MD clearly demonstrated that cellular homeostasis was maintained by intricate and inter-connected signaling and metabolic pathways. Limitation of a single nutrient, such as methionine, would likely be sensed and trigger cascades of signaling and metabolic consequences and disrupt homeostasis.

Author contributions

G. H. and K. M. designed the research; H. J., F. B., X. W., and K. W. conducted the experiments; F. B. and H. Z. analyzed the data; G. H. and H. J. wrote the manuscript. All authors read and approved the final manuscript.

Appendix A. Supplementary Data

Supplementary data to this article can be found online at http://dx.doi.org/10.1016/j.jnutbio.2017.08.015.

References

[1] Kozak M. Comparison of initiation of protein synthesis in procaryotes, eucaryotes, and organelles. Microbiol Rev 1983;47:1–45.
[2] Brosnan JT, Brosnan ME. The sulfur-containing amino acids: an overview. J Nutr 2006;136:1636S–40S.
[3] Solberg J, Buttery P, Boorman K. Effect of moderate methionine deficiency on food, protein and energy utilisation in the chick. Br Poult Sci 1971;12:297–304.
[4] Sekiz SS, Scott ML, Nesheim MC. The effect of methionine deficiency on body weight, food and energy utilization in the chick. Poult Sci 1975;54:1184–8.
[5] Barnes DM, Calvert CC, Klasing KC. Methionine deficiency decreases protein accretion and synthesis but not tRNA acylation in muscles of chicks. J Nutr 1995; 125:2623–30.
[6] Bauchart-Thevret C, Stoll B, Chacko S, Burrin DG. Sulfur amino acid deficiency upregulates intestinal methionine cycle activity and suppresses epithelial growth in neonatal pigs. Am J Physiol Endocrinol Metab 2009;296:E1239–50.
[7] Castellano R, Perruchot M-H, Conde-Aguilera JA, van Milgen J, Collin A, Tesseraud S, et al. A methionine deficient diet enhances adipose tissue lipid metabolism and alters anti-oxidant pathways in young growing pigs. PLoS One 2015;10: e0130514.
[8] Conde-Aguilera JA, Lefaucheur L, Tesseraud S, Mercier Y, Le Floc'h N, van Milgen J. Skeletal muscles respond differently when piglets are offered a diet 30% deficient in total sulfur amino acid for 10 days. Eur J Nutr 2016;55:117–26.
[9] Tang Y, Tan B, Xiong X, Li F, Ren W, Kong X, et al. Methionine deficiency reduces autophagy and accelerates death in intestinal epithelial cells infected with enterotoxigenic *Escherichia coli*. Amino Acids 2015;47:2199–204.
[10] Tang Y, Li F, Tan B, Liu G, Kong X, Hardwidge PR, et al. Enterotoxigenic *Escherichia coli* infection induces intestinal epithelial cell autophagy. Vet Microbiol 2014;171: 160–4.
[11] Walton MJ, Cowey CB, Adron JW. Methionine metabolism in rainbow trout fed diets of differing methionine and cystine content. J Nutr 1982;112:1525–35.
[12] Keembiyehetty CN, Gatlin DM. Total sulfur amino acid requirement of juvenile hybrid striped bass (*Morone chrysops*× *M. saxatilis*). Aquaculture 1993;110:331–9.
[13] Simmons L, Moccia R, Bureau D, Sivak J, Herbert K. Dietary methionine requirement of juvenile Arctic charr *Salvelinus alpinus* (L.). Aquacult. Nutrition 1999;5:93–100.
[14] Tulli F, Messina M, Calligaris M, Tibaldi E. Response of European sea bass (*Dicentrarchus labrax*) to graded levels of methionine (total sulfur amino acids) in soya protein-based semi-purified diets. Br J Nutr 2010;104:664–73.
[15] Hardy RW. Utilization of plant proteins in fish diets: effects of global demand and supplies of fishmeal. Aquac Res 2010;41:770–6.
[16] Clarke S, Banfield K. S-adenosylmethionine-dependent methyltransferases. Homocysteine in health and disease; 2001. p. 63–78.
[17] Fontecave M, Atta M, Mulliez E. S-adenosylmethionine: nothing goes to waste. Trends Biochem Sci 2004;29:243–9.
[18] Mato JM, Martínez-Chantar ML, Lu SC. Methionine metabolism and liver disease. Annu Rev Nutr 2008;28:273–93.
[19] Pegg AE. Mammalian polyamine metabolism and function. IUBMB Life 2009;61: 880–94.
[20] Efeyan A, Comb WC, Sabatini DM. Nutrient-sensing mechanisms and pathways. Nature 2015;517:302–10.
[21] Yao K, Yin Y-L, Chu W, Liu Z, Deng D, Li T, et al. Dietary arginine supplementation increases mTOR signaling activity in skeletal muscle of neonatal pigs. J Nutr 2008; 138:867–72.
[22] Li F, Yin Y, Tan B, Kong X, Wu G. Leucine nutrition in animals and humans: mTOR signaling and beyond. Amino Acids 2011;41:1185–93.
[23] Yin Y, Yao K, Liu Z, Gong M, Ruan Z, Deng D, et al. Supplementing L-leucine to a low-protein diet increases tissue protein synthesis in weanling pigs. Amino Acids 2010;39:1477–86.
[24] Tan Be, Xiao H, Xiong X, Wang J, Li G, Yin Y, et al. L-arginine improves DNA synthesis in LPS-challenged enterocytes. Front Biosci (Landmark Ed) 2014;20: 989–1003.
[25] Kim J, Guan K-L. Amino acid signaling in TOR activation. Annu Rev Biochem 2011; 80:1001–32.
[26] Laplante M, Sabatini DM. mTOR signaling in growth control and disease. Cell 2012;149:274–93.
[27] Hotamisligil GS, Erbay E. Nutrient sensing and inflammation in metabolic diseases. Nat Rev Immunol 2008;8:923–34.
[28] Gallinetti J, Harputlugil E, Mitchell JR. Amino acid sensing in dietary-restriction-mediated longevity: roles of signal-transducing kinases GCN2 and TOR. Biochem J 2013;449:1–10.
[29] Chaveroux C, Lambert-Langlais S, Cherasse Y, Averous J, Parry L, Carraro V, et al. Molecular mechanisms involved in the adaptation to amino acid limitation in mammals. Biochimie 2010;92:736–45.
[30] Düvel K, Yecies JL, Menon S, Raman P, Lipovsky AI, Souza AL, et al. Activation of a metabolic gene regulatory network downstream of mTOR complex 1. Mol Cell 2010;39:171–83.
[31] Xu D, He G, Mai K, Zhou H, Xu W, Song F. Postprandial nutrient-sensing and metabolic responses after partial dietary fishmeal replacement by soyabean meal in turbot (*Scophthalmus maximus L.*). Br J Nutr 2016;115:379–88.
[32] Song F, Xu D, Mai K, Zhou H, Xu W, He G. Comparative study on the cellular and systemic nutrient sensing and intermediary metabolism after partial replacement of fishmeal by meat and bone meal in the diet of turbot (*Scophthalmus maximus L.*). PLoS One 2016;11:e0165708.
[33] Seiliez I, Panserat S, Lansard M, Polakof S, Plagnes-Juan E, Surget A, et al. Dietary carbohydrate-to-protein ratio affects TOR signaling and metabolism-related gene expression in the liver and muscle of rainbow trout after a single meal. Am J Phys Regul Integr Comp Phys 2011;300:R733–43.
[34] Belghit I, Skiba-Cassy S, Geurden I, Dias K, Surget A, Kaushik S, et al. Dietary methionine availability affects the main factors involved in muscle protein turnover in rainbow trout (*Oncorhynchus mykiss*). Br J Nutr 2014;112:493–503.
[35] Vélez EJ, Lutfi E, Jiménezamilburu V, Rieracodina M, Capilla E, Navarro I, et al. IGF-I and amino acids effects through TOR signaling on proliferation and differentiation of gilthead sea bream cultured myocytes. Gen Comp Endocrinol 2014;205: 296–304.
[36] Bian F, Jiang H, Man M, Mai K, Zhou H, Xu W, et al. Dietary gossypol suppressed postprandial TOR signaling and elevated ER stress pathways in turbot (*Scophthal-*.). *Am J Physiol Endocrinol Metab 2017;312(1):E37–47.*
[37] Joyce AR, Palsson BØ. The model organism as a system: integrating 'omics' data sets. Nat Rev Mol Cell Biol 2006;7:198–210.
[38] Kussmann M, Rezzi S, Daniel H. Profiling techniques in nutrition and health research. Curr Opin Biotechnol 2008;19:83–99.
[39] Kussmann M, Panchaud A, Affolter M. Proteomics in nutrition: status quo and outlook for biomarkers and bioactives. J Proteome Res 2010;9:4876–87.
[40] Martin SA, Vilhelmsson O, Médale F, Watt P, Kaushik S, Houlihan DF. Proteomic sensitivity to dietary manipulations in rainbow trout. Biochim Biophys Acta 1651; 2003:17–29.
[41] Jury DR, Kaveti S, Duan ZH, Willard B, Kinter M, Londraville R. Effects of calorie restriction on the zebrafish liver proteome. Comp Biochem Physiol Part D Genomics Proteomics 2008;3:275–82.
[42] Sissener NH, Martin SAM, Cash P, Hevrøy EM, Sanden M, Hemre GI. Proteomic profiling of liver from atlantic salmon (*Salmo salar*) fed genetically modified soy compared to the near-isogenic non-GM line. Mar Biotechnol (NY) 2010;12: 273–81.
[43] Gómez-Requeni P, De VM, Kousoulaki K, Jordal AE, Conceição LE, Rønnestad I. Whole body proteome response to a dietary lysine imbalance in zebrafish *Danio rerio*. Comp Biochem Physiol Part D Genomics Proteomics 2011;6:178–86.
[44] Craig PM, Moon TW. Methionine restriction affects the phenotypic and transcriptional response of rainbow trout (*Oncorhynchus mykiss*) to carbohydrate-enriched diets. Br J Nutr 2013;109:402–12.
[45] Boeuf G, Payan P. How should salinity influence fish growth? Comp Biochem Physiol C Toxicol Pharmacol 2001;130:411–23.
[46] Olivateles A. Nutrition and health of aquaculture fish. J Fish Dis 2012;35:83–108.
[47] Yamamoto T, Shima T, Furuita H, Suzuki N, Sánchez-Vázquez FJ, Tabata M. Self-selection and feed consumption of diets with a complete amino acid composition and a composition deficient in either methionine or lysine by rainbow trout, *Oncorhynchus mykiss* (Walbaum). Aquac Res 2001;32:83–91.
[48] Wei Y, He G, Mai K, Xu W, Zhou H, Mei L. Apparent digestibility of selected feed ingredients in juvenile turbot (*Scophthalmus maxima L.*). Isr J Aquacult-Bamid 2015;67:1173 http://hdl.handle.net/10524/49191.
[49] Lansard M, Panserat S, Plagnesjuan E, Dias K, Seiliez I, Skibacassy S. L-leucine, L-methionine, and L-lysine are involved in the regulation of intermediary metabolism-related gene expression in rainbow trout hepatocytes. J Nutr 2011; 141:75–80.
[50] Dai W, Panserat S, Plagnes-Juan E, Seiliez I, Skiba-Cassy S. Amino acids attenuate insulin action on gluconeogenesis and promote fatty acid biosynthesis via mtorc1 signaling pathway in trout hepatocytes. Cell Physiol Biochem 2015;36:1084–100.
[51] Wang X, He G, Mai K, Xu W, Zhou H. Molecular cloning and characterization of taurine transporter from turbot (*Psetta maxima*) and its expression analysis regulated by taurine in vitro. Aquac Res 2017;48:1724–34.
[52] Xu C, Gao X, Sun X, Wen CK. The basal level ethylene response is important to the wall and endomembrane structure in the hypocotyl cells of etiolated Arabidopsis seedlings. J Integr Plant Biol 2012;54:434–55.
[53] Zuo R, Ai Q, Mai K, Xu W, Wang J, Xu H, et al. Effects of dietary n-3 highly unsaturated fatty acids on growth, nonspecific immunity, expression of some immune related genes and disease resistance of large yellow croaker (*Larmichthys crocea*) following natural infestation of parasites (*Cryptocaryon irritans*). Fish Shellfish Immunol 2012;32:249–58.
[54] Livak KJ, Schmittgen TD. Analysis of relative gene expression data using real-time quantitative PCR and the 2− ΔΔCT method. Methods 2001;25:402–8.
[55] Wang Q, He G, Mai K, Xu W, Zhou H, Wang X, et al. Chronic rapamycin treatment on the nutrient utilization and metabolism of juvenile turbot (*Psetta maxima*). Sci Rep 2016;6:28068.
[56] Altman MK, Alshamrani AA, Jia W, Nguyen HT, Fambrough JM, Tran SK, et al. Suppression of the GTPase-activating protein RGS10 increases Rheb-GTP and mTOR signaling in ovarian cancer cells. Cancer Lett 2015;369:175–83.
[57] Tabit CE, Shenouda SM, Monica H, Fetterman JL, Soroosh K, Frame AA, et al. Protein kinase C-β contributes to impaired endothelial insulin signaling in humans with diabetes mellitus. Circulation 2013;127:86–95.
[58] Chen R, Zou Y, Mao D, Sun D, Gao G, Shi J, et al. The general amino acid control pathway regulates mTOR and autophagy during serum/glutamine starvation. J Cell Biol 2014;206:173–82.

[59] Xia X, Che Y, Gao Y, Zhao S, Ao C, Yang H, et al. Arginine supplementation recovered the ifn-γ-mediated decrease in milk protein and fat synthesis by inhibiting the GCN2/eIF2α pathway, which induces autophagy in primary bovine mammary epithelial cells. Mol Cell 2016;39:410–7.
[60] Kang Q, Chen A. Curcumin suppresses expression of low-density lipoprotein (LDL) receptor, leading to the inhibition of LDL-induced activation of hepatic stellate cells. Br J Pharmacol 2009;157:1354–67.
[61] Will Y, Hynes J, Ogurtsov VI, Papkovsky DB. Analysis of mitochondrial function using phosphorescent oxygen-sensitive probes. Nat Protoc 2006;1:2563–72.
[62] Ye J, Palm W, Peng M, King B, Lindsten T, Li MO, et al. GCN2 sustains mTORC1 suppression upon amino acid deprivation by inducing Sestrin2. Genes Dev 2015;29:2331–6.
[63] Sigauke E, Rakheja D, Kitson K, Bennett MJ. Carnitine palmitoyltransferase II deficiency: a clinical, biochemical, and molecular review. Lab Investig 2003;83:1543–54.
[64] Reddy JK, Hashimoto T. Peroxisomal β-oxidation and peroxisome proliferator-activated receptor α: an adaptive metabolic system. Annu Rev Nutr 2001;21:193–230.
[65] Cunha I, Galante-Oliveira S, Rocha E, Planas M, Urbatzka R, Castro L. Dynamics of PPARs, fatty acid metabolism genes and lipid classes in eggs and early larvae of a teleost. Comp Biochem Physiol B Biochem Mol Biol 2013;164:247–58.
[66] Louassini M, Foulquié M, Benítez R, Adroher J. Citric-acid cycle key enzyme activities during in vitro growth and metacyclogenesis of *Leishmania* infantum promastigotes. J Parasitol 1999;85:595–602.
[67] Wang Z, Mai K, Xu W, Zhang Y, Liu Y, Ai Q. Dietary methionine level influences growth and lipid metabolism via GCN2 pathway in cobia (*Rachycentron canadum*). Aquaculture 2016;454:148–56.
[68] Figueiredo-Silva C, Lemme A, Sangsue D, Kiriratnikom S. Effect of DL-methionine supplementation on the success of almost total replacement of fish meal with soybean meal in diets for hybrid tilapia (*Oreochromis niloticus*× *Oreochromis mossambicus*). Aquac Nutr 2015;21:234–41.
[69] Kilberg MS, Shan J, Su N. ATF4-dependent transcription mediates signaling of amino acid limitation. Trends Endocrinol Metab 2009;20:436–43.
[70] Skiba-Cassy S, Geurden I, Panserat S, Seiliez I. Dietary methionine imbalance alters the transcriptional regulation of genes involved in glucose, lipid and amino acid metabolism in the liver of rainbow trout (*Oncorhynchus mykiss*). Aquaculture 2016;454:56–65.
[71] Kim JS, Ro S-H, Kim M, Park H-W, Semple IA, Park H, et al. Sestrin2 inhibits mTORC1 through modulation of GATOR complexes. Sci Rep 2015;5:9502.
[72] Wek RC, Jiang HY, Anthony TG. Coping with stress: eIF2 kinases and translational control. Biochem Soc Trans 2006;34:7–11.
[73] Hardie D. AMPK: a key regulator of energy balance in the single cell and the whole organism. Int J Obes 2008;32:S7–S12.
[74] Hardie DG, Ross FA, Hawley SA. AMPK: a nutrient and energy sensor that maintains energy homeostasis. Nat Rev Mol Cell Biol 2012;13:251–62.
[75] Martínez-Chantar ML, Vázquez-Chantada M, Garnacho M, Latasa MU, Varela-Rey M, Dotor J, et al. S-Adenosylmethionine regulates cytoplasmic HuR via AMP–activated kinase. Gastroenterology 2006;131:223–32.
[76] Wortham M, He L, Gyamfi M, Copple BL, Wan Y-JY. The transition from fatty liver to NASH associates with SAMe depletion in db/db mice fed a methionine choline-deficient diet. Dig Dis Sci 2008;53:2761–74.
[77] Lee JH, Budanov AV, Karin M. Sestrins orchestrate cellular metabolism to attenuate aging. Cell Metab 2013;18:792–801.
[78] Stoka V, Turk V, Turk B. Lysosomal cathepsins and their regulation in aging and neurodegeneration. Ageing Res Rev 2016;32:22–37.
[79] Seiliez I, Panserat S, Skibacassy S, Fricot A, Vachot C, Kaushik S, et al. Feeding status regulates the polyubiquitination step of the ubiquitin-proteasome-dependent proteolysis in rainbow trout (*Oncorhynchus mykiss*) muscle. J Nutr 2008;138: 487–91.
[80] Guo F, Cavener DR. The GCN2 eIF2alpha kinase regulates fatty-acid homeostasis in the liver during deprivation of an essential amino acid. Cell Metab 2007;5:103–14.
[81] Lunt SY, Heiden MGV. Aerobic glycolysis: meeting the metabolic requirements of cell proliferation. Annu Rev Cell Dev Biol 2011;27:441–64.
[82] Ježek P, Engstová H, Žáčková M, Vercesi AE, Costa AD, Arruda P, et al. Fatty acid cycling mechanism and mitochondrial uncoupling proteins. Biochim Biophys Acta 1998;1365:319–27.
[83] Matthias A, Jacobsson A, Cannon B, Nedergaard J. The bioenergetics of brown fat mitochondria from UCP1-ablated mice. Ucp1 is not involved in fatty acid-induced de-energization ("uncoupling"). J Biol Chem 1999;274:28150–60.
[84] Devi SL, Anuradha C. Mitochondrial damage, cytotoxicity and apoptosis in iron-potentiated alcoholic liver fibrosis: amelioration by taurine. Amino Acids 2010; 38:869–79.
[85] Wanders D, Burk DH, Cortez CC, Van NT, Stone KP, Baker M, et al. UCP1 is an essential mediator of the effects of methionine restriction on energy balance but not insulin sensitivity. FASEB J 2015;29:2603–15.